Photoemission Study of Onion Like Quantum Dot Quantum Well and Double Quantum Well Nanocrystals of CdS and HgS†

Holger Borchert,*,‡ Dirk Dorfs,‡ Colm McGinley,§ Sorin Adam,§ Thomas Möller,§ Horst Weller,‡ and Alexander Eychmüller‡

Institute of Physical Chemistry, University of Hamburg, Bundesstr. 45, 20146 Hamburg, Germany, and Hamburger Synchrotronstrahlungslabor HASYLAB at DESY, Notkestr. 85, 22603 Hamburg, Germany

Received: November 18, 2002; In Final Form: January 30, 2003

Colloidally prepared CdS/HgS/CdS quantum dot quantum well nanocrystals and CdS/HgS/CdS/HgS/CdS double quantum well nanocrystals stabilized with polyphosphates have been investigated by photoelectron spectroscopy with tuneable synchrotron radiation. High-resolution spectra reveal in addition to a bulk species also a surface environment for Cd, whereas different S species could not be resolved. Although not expected for the ideal structure model, Hg occurs in two distinct environments. The total amount of Hg giving evidence for sample inhomogeneities is of the order of 10%. Furthermore, to some extent, the XPS experiments allowed characterization of the onion like structure of the quantum dot quantum well nanocrystals. A method for layer thickness determination previously developed for core shell nanocrystals is extended to the more complex case of quantum dot quantum well structures.

1. Introduction

An important field in nanotechnology is the fabrication of composite structures comprising different semiconductor materials. Chemically grown quantum dots can be coated with a shell of another material by various overgrowth methods. This gives rise to so-called core−shell nanocrystals.[1−3] Examples are CdS/$Cd(OH)_2$,[4] CdSe/CdS,[5] CdSe/ZnS,[6,7] or InAs nanocrystals coated with different II−IV and III−V shell materials.[8] Multiple application of the growth techniques enables the addition of further shells to create quantum dot quantum well structures which are also referred to as nano-onions.[9] In CdS/HgS/CdS nanocrystals, a well of HgS is embedded between a CdS core and an outer shell of CdS.[10,11] Recently, even more complex structures have been synthesized. In CdS/HgS/CdS/HgS/CdS double quantum well nanocrystals, two separated wells of HgS are embedded in CdS.[12,13]

A useful contribution to the structural analysis and complete description of such composite nanocrystals can be provided by photoelectron spectroscopy with tuneable synchrotron radiation. By tuning the energy, it is possible to vary the surface sensitivity of the experiment and thus to reveal information about the nanocrystal surface and to analyze the composition of the nanoparticles as a function of depth. High resolution photoelectron spectroscopy has successfully been used to identify distinct surface environments for example in CdS[14−17] and InAs nanocrystals.[18] Recently, it was demonstrated for InP/ZnS,[19] InAs/CdSe,[20] and CdSe/ZnS[21] core−shell nanocrystals that the average thickness of the overgrown shell may be determined provided the core diameter is known.

In this study, we investigate quantum well and double quantum well nanostructures of CdS and HgS with the aim of obtaining information about the surface of the composite nanocrystals and to examine how far the method already developed for shell thickness determination in core−shell nanocrystals can be extended to more complex structures.

2. Experimental Section

2.1. Preparation. CdS nanocrystals have been prepared according to a method described in the literature where H_2S is injected into the gas phase above an aqueous solution of $Cd(ClO_4)_2$.[4] Sodium polyphosphates are used as stabilizer in this procedure.

To obtain onion like quantum dot quantum well particles, several steps are necessary.[22] First, the addition of an appropriate amount of $Hg(ClO_4)_2$ leads to the substitution of the surface Cd atoms by Hg. Next, the Cd^{2+} ions released into the solution can be reattached as CdS to the nanocrystal surface by addition of H_2S. At that stage, the nanocrystals are comprised of a CdS core, one monolayer of HgS, and again one monolayer of CdS. Repetitive addition of $Hg(ClO_4)_2$ and H_2S further increases the thickness of the HgS shell by replacing again the outermost CdS layer by HgS, followed by termination of the nanocrystals with a new CdS layer. Finally, additional CdS is overgrown onto the nanocrystals. Therefore, $Cd(ClO_4)_2$ and H_2S are added. Details of the synthesis are reported in the literature.[22]

For the double quantum dot quantum well nanocrystals, the above procedure can simply be applied again.[13] The thickness of the different shells in the composite nanocrystals is governed by the amounts of $Cd(ClO_4)_2$ and $Hg(ClO_4)_2$ used in the different steps of the synthesis, respectively. The CdS/HgS/CdS quantum dot quantum well particles investigated in this study should ideally possess a CdS core covered by 2 monolayers of HgS and 3 monolayers of again CdS. Also, the double quantum well nanocrystals should have two times 2 and 3 monolayers of HgS and CdS, respectively, where a monolayer is defined as the half of the cubic lattice parameter, i.e., 0.29 nm. Note here that the above description depicts ideal structures. As discussed in the literature,[13,22] a certain degree of intermixing and thickness

† Part of the special issue "Arnim Henglein Festschrift".

* To whom correspondence should be addressed. E-mail: Holger_Borchert@public.uni-hamburg.de. Fax: +49-40-42838-3452.

‡ University of Hamburg.

§ Hamburger Synchrotronstrahlungslabor HASYLAB at DESY.

10.1021/jp027485t CCC: $25.00
Published on Web 03/01/2003

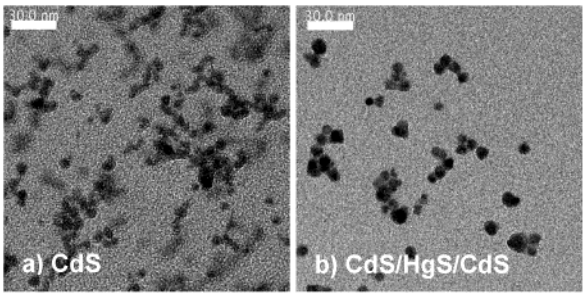

Figure 1. Transmission electron micrographs of CdS (a) and CdS/HgS/CdS quantum dot quantum well nanocrystals (b)

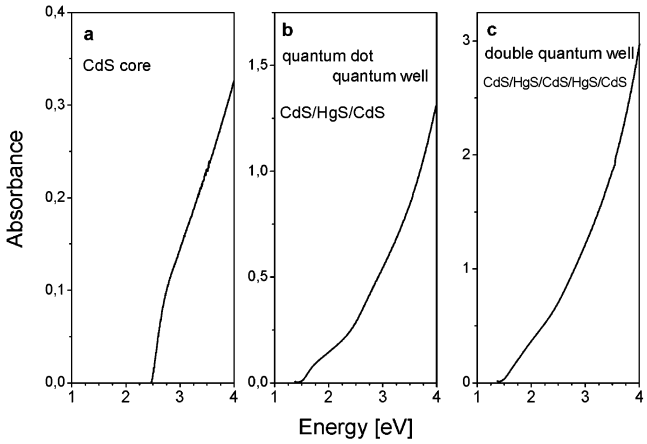

Figure 2. Absorption spectra of CdS (a), CdS/HgS/CdS quantum dot quantum well (b), and CdS/HgS/CdS/HgS/CdS double quantum well nanocrystals (c)

variations in the different shells are certainly to be expected in the real samples.

2.2. Optical Characterization and Transmission Electron Microscopy. Figure 1 shows transmission electron micrographs (TEM images) of the initial CdS nanocrystals and the CdS/HgS/CdS quantum dot quantum well particles. The CdS nanocrystals have an average diameter of 5.3 nm with a standard deviation of about 20%. The size distribution remains similarly narrow after overgrowth of the HgS and CdS shells. The average size of 7.8 nm for the quantum dot quantum well nanocrystals is in good agreement with the expected value of 7.7 nm. (From the core diameter of 5.3 nm have to be subtracted 0.6 nm for the outermost CdS layer which is replaced by HgS when 2 monolayers of HgS and 3 monolayers of CdS are overgrown.)

Absorption spectra of the CdS cores, quantum dot quantum well, and double quantum well particles are presented in Figure 2.

2.3. Photoelectron Spectroscopy. Photoemission experiments were performed at beamline BW3 at the synchrotron source at HASYLAB/DESY in Hamburg, Germany. Spectra have been recorded in normal emission mode with an Omicron EA 125 hemispherical electron analyzer orientated at 45° to the incident beam.

The synchrotron energy was tuned in the range from 200 to 1500 eV. Variation of the excitation energy changes the kinetic energy of the generated photoelectrons. Because the mean free path length of electrons in matter depends on their kinetic energy, this influences the attenuation of photoemission peak intensities due to scattering of the photoelectrons in the sample. The mean free path length has a minimum around a kinetic energy of about ~50 eV.[23] If the synchrotron energy is adjusted to these conditions for a given photoemission peak, mainly, the surface atoms contribute to the signal. When the synchrotron energy is then increased, the mean free path length also increases and electrons emitted deeper inside the sample contribute more and more to the signal. Based on this principle, it is possible to vary the surface sensitivity of the experiment.

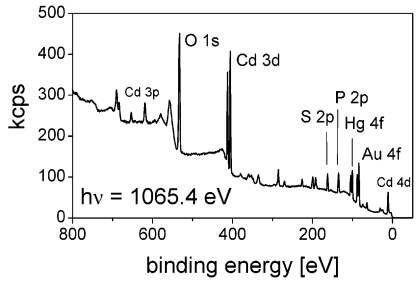

Figure 3. Overview spectrum of the CdS/HgS/CdS quantum dot quantum well nanocrystals at high excitation energy

To prepare the samples for the XPS measurements, nanocrystals were deposited from aqueous solution onto thin gold foils. An exicator was used to evaporate the solvent. Several drops were placed one after another. Figure 3 shows an XPS overview spectrum of the CdS/HgS/CdS quantum dot quantum well particles recorded at high excitation energy. One can see different core levels of Cd, Hg, and S. Further, P and O from the polyphosphate stabilizer are visible. Note also the presence of the Au 4f level. To prevent charging of the sample, we had to work with low concentrations of nanocrystals on the substrate. We have concentrated our study on the Cd $3d_{5/2}$, S 2p and the Hg 4f core levels. High-resolution spectra have been fitted with Voigt profiles.

3. Results and Discussion

3.1. Study of the Cd $3d_{5/2}$ Level in CdS/HgS/CdS. Spectra of the Cd $3d_{5/2}$ level in CdS/HgS/CdS quantum dot quantum well nanocrystals have been recorded at a series of excitation energies in the range from 500 to 1500 eV. Figure 4a shows a spectrum recorded at a surface sensitive energy with a total experimental resolution of about 0.3 eV. The experimental curve is plotted together with an attempt to fit the spectrum using a polynomial background and one single Voigt function. As indicated by the residual plot, this fit is rather poor. The spectrum obviously has a small shoulder on the high binding energy side. Figure 4b shows the same spectrum fitted with two Voigt functions. The Gaussian width are 0.70 and 0.95 eV for the components labeled "V" and "S", respectively. The Lorentzian width was constrained to be identical for both components and is 0.32 eV in the presented fit. The chemical shift between the two components is 0.38 eV. This value turned out to be rather independent of the degree of the polynomial background function used. Also, liberating the constraint for equal Lorentzian width or fixing the Lorentzian width to the value of 0.38 eV found for the Cd 3d level in the literature[24] affect the fit only very slightly.

Nevertheless, care has to be taken as to the reliability of the above results. The shoulder on the high binding energy side is not pronounced enough to appear as a well resolved feature in the spectrum, and normally unambiguous fitting of core level spectra requires the consistent fitting of a series of spectra recorded in a wide range of excitation energies. This is however difficult here, because at higher energy the experimental resolution decreases further. Figure 4c shows a spectrum recorded at 770 eV. Here, the experimental resolution is about 0.44 eV; that is, it reaches the order of the chemical shift in question. Obviously, although still present, the shoulder is now much less pronounced and the spectrum can nearly be fitted

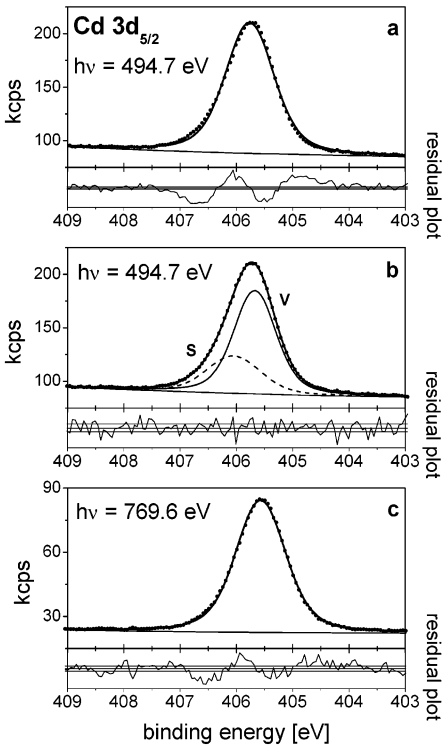

Figure 4. High-resolution spectra of the Cd $3d_{5/2}$ core level of CdS/HgS/CdS quantum dot quantum well nanocrystals. At lower energy, fitting with one single Voigt function is insufficient (a), a second component is required (b). "S" corresponds to Cd atoms at the surface, and "V" corresponds to Cd atoms in the volume of the nanocrystals. At higher energy, the two components cannot be resolved (c).

with a single component. If two components are used, the convergence is much worse than for the spectrum in Figure 4b. The value of the chemical shift is no longer independent of the background function used. This makes reliable fitting at higher energies impossible.

As a consequence, the observation of the two components relies here mainly on spectra recorded at surface sensitive energies. In the range from 500 to 600 eV, three spectra have been recorded and the value of the observed chemical shift varied between 0.32 and 0.38 eV. Because the spectra appear very similar, only one of them is presented in Figure 4b. Fixing the chemical shift and Lorentzian width to identical values for all three spectra allows comparison of the intensity ratio between the two components. The ratio turned out to be slightly increasing in favor of the component labeled "S" from 0.37 at 590 eV to 0.50 at the more surface sensitive energy of 495 eV. Therefore, the component "S" can be attributed to Cd atoms at the nanoparticle surface, whereas the component "V" corresponds to Cd atoms in the volume of the particles. Although the energy range where reliable fitting with two components is possible is rather narrow here, the identification of the two components with a chemical shift of about 0.4 eV is still justified. Note also that the surface component "S" has a higher Gaussian width than the volume component "V". Slightly different surface sites lead to an additional broadening.

3.2. Study of the S 2p Level in CdS/HgS/CdS. S 2p spectra have been recorded at a series of energies in the range from 230 to 1500 eV. Figure 5 shows a spectrum at a surface sensitive energy. A Shirley-type background function that takes care of the step like background increase at the photoemission peak and one spin−orbit split doublet of Voigt functions lead to a reasonable fit. Note especially that the quality of the fit cannot be considerably improved here by using two or three doublets.

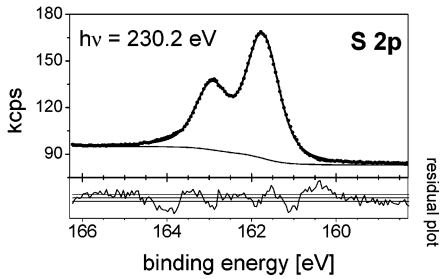

Figure 5. High resolution spectrum of the S 2p core level of CdS/HgS/CdS nanocrystals at a surface sensitive energy. Only one spin−orbit split doublet of Voigt functions is required to obtain a reasonable fit.

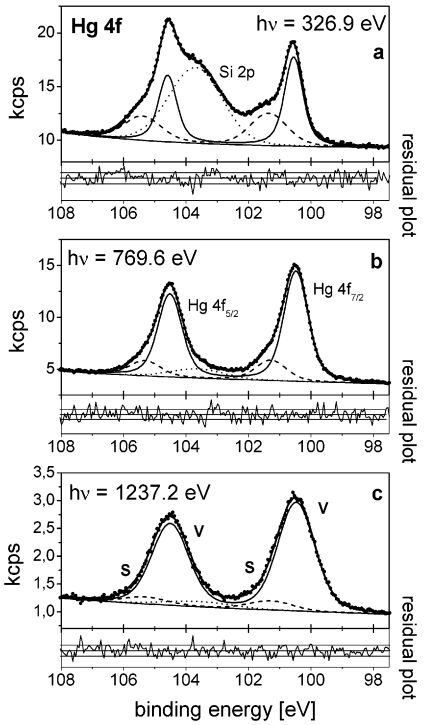

Figure 6. High-resolution spectra of the Hg 4f core level of CdS/HgS/CdS nanocrystals. Two spin−orbit split components plotted as solid and dashed lines are visible. The Hg 4f spectra overlap with a Si 2p signal plotted as dotted line.

Only one sulfur species is observed. The binding energy of 161.8 eV ± 0.1 eV for the $2p_{3/2}$ sublevel is in good agreement with the binding energy of the S $2p_{3/2}$ level measured in bulk CdS.[25,26] Neither is it possible in our spectra to distinguish between S in CdS and in HgS nor can a distinct surface environment be seen.

3.3. Study of the Hg 4f Level in CdS/HgS/CdS. Hg 4f spectra have been recorded in the range from 230 to 1500 eV. Three spectra are presented in Figure 6. Two spin−orbit split components plotted as solid and dashed lines respectively are visible. The Hg 4f signal overlaps with the 2p level of Si which is an impurity in the sample and probably originates from the glass instruments used in the synthesis of the nanoparticles. Especially at low energy, the Si 2p signal seems huge, but note that the intensity of the Hg 4f peaks is strongly attenuated by the surrounding CdS shell. The shift between the two Hg 4f components is 0.8 eV and the relative intensity of the component labeled "S" increases at more surface sensitive energies. This component therefore corresponds to Hg in a surface environment. This result is not to be expected for a perfect quantum well structure comprised of two monolayers of HgS embedded in CdS. In the ideal case, all of the Hg atoms should be nearly

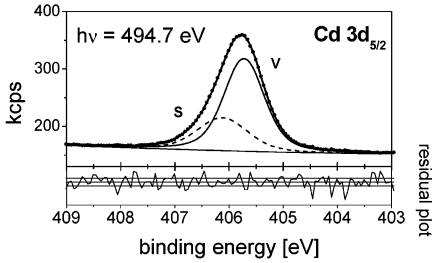

Figure 7. High-resolution spectrum of the Cd $3d_{5/2}$ core level in the CdS/HgS/CdS/HgS/CdS double quantum well nanocrystals. Two Voigt functions are necessary to obtain a good fit.

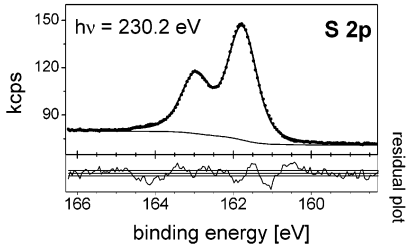

Figure 8. High resolution spectrum of the S 2p core level of CdS/HgS/CdS/HgS/CdS double quantum well nanocrystals at a surface sensitive energy. Only one spin−orbit split doublet of Voigt functions is required to obtain a reasonable fit.

identical with four S neighbors for each Hg atom, and only one spin−orbit split Hg 4f peak should be observed. The presence of the second species confirms that real samples present indeed some inhomogeneities.

Different explanations for the existence of the second component are to be considered. One possibility is a certain degree of disorder at the interface between CdS and HgS which might lead to another environment for Hg. Furthermore, we cannot exclude the possibility that the HgS layer is not completely covered by the outer CdS layer. Finally, the second component could be due to the formation of small HgS or $Hg_xCd_{1-x}S$ clusters which might be formed as a byproduct in the synthesis of the quantum dot quantum well nanocrystals. At a first look, the relative intensity of the component "S" seems to be quite large, because the intensity of the component "V" corresponding to Hg atoms in the HgS quantum well is attenuated by the surrounding CdS shell. Assuming a CdS shell of ∼1 nm thickness and that the component "S" corresponds to a surface species of Hg atoms, one can estimate that about 10% of Hg is not incorporated according to the ideal structure. This result seems to be reasonable having in mind the complex synthesis of the composite nanocrystals.

3.4. Core Level Studies in CdS/HgS/CdS/HgS/CdS. As is to be expected, the photoemission spectra of the CdS/HgS/CdS/HgS/CdS double quantum well nanocrystals look quite similar to those of the single well species. Figure 7 shows a high-resolution spectrum of the Cd $3d_{5/2}$ core level at a surface sensitive energy. Again two components with a chemical shift of 0.4 eV are visible. The Gaussian and Lorentzian width are similar to the values found for the CdS/HgS/CdS quantum well particles. Also for the intensity ratios there is no major difference. The ratio of component "S" to component "V" increases from 0.38 to 0.45 in the energy range from 590 to 495 eV.

The S 2p spectra are again fittable with one spin−orbit split doublet of Voigt functions as can be seen in Figure 8. Also here only one sulfur species is observable.

Qualitatively also the Hg 4f spectra presented in Figure 9 resemble those of the CdS/HgS/CdS quantum well particles.

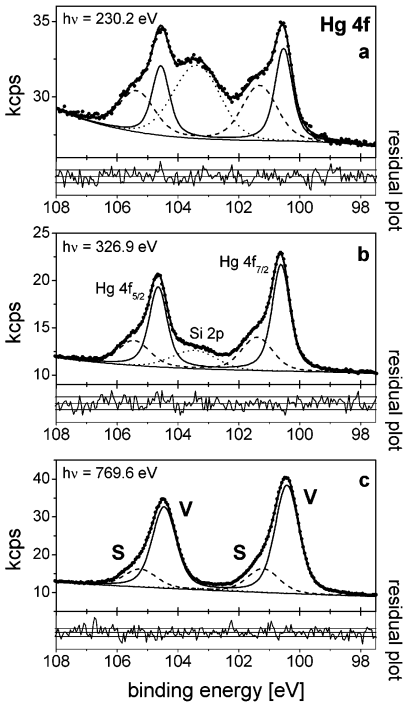

Figure 9. High-resolution spectra of the Hg 4f core level of CdS/HgS/CdS/HgS/CdS nanocrystals. Two spin−orbit split components plotted as solid and dashed lines are visible. The Hg 4f spectra overlap with a Si 2p signal plotted as dotted line.

The amount of Si is lower in the second sample, and the percentage of Hg which does not conform to the ideal structure is again of the order of 10%.

3.5. Quantum Well Structure of CdS/HgS/CdS. On the basis of the principle of varying the surface sensitivity of the photoemission experiment by tuning the synchrotron energy, it is possible to examine the onion like structure of the composite nanocrystals. In the case of core−shell nanocrystals, one can determine the average thickness of the overgrown shell, if the core diameter is known.[19−21] Therefore, spectra of elements associated uniquely with the core or the shell are recorded at a series of energies. Peak intensities are measured and normalized taking several factors into account, namely the beam intensity, the photoionization cross-section, an asymmetry term taking care of the geometry of the experiment and the energy dependent sensitivity function of the electron analyzer.[19−21] The normalized intensity of a given peak should then be proportional to the following integral over the sample structure:

$$I_{\mathrm{norm}} \propto \int_{\mathrm{sample}} \mathrm{d}V\, \rho(\bar{\mathbf{r}})\, \mathrm{e}^{-d(\bar{\mathbf{r}})/\lambda(E_{\mathrm{kin}})} \qquad (1)$$

Here ρ is the atomic density of the element in question and the exponential function describes the signal attenuation due to scattering. d is the distance a photoelectron emitted at $\mathbf{r}$ has to pass through the sample before detection and λ is the mean free path length.

Assuming a spherical geometry for the core shell nanocrystals theoretical intensities may easily be calculated and compared to the experimental intensities. Variation of the shell thickness in the calculation enables determination of the average thickness of the overgrown shell by a least-squares fit.[19]

This method works quite well for core shell nanocrystals, and it is of interest to examine, if and how far it can be extended to the more complex case of quantum dot quantum well nanocrystals. Thus, we have performed a quantitative analysis

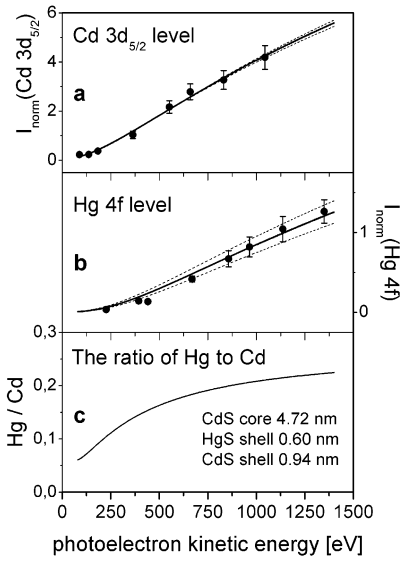

Figure 10. Normalized intensities of the Cd $3d_{5/2}$ (a) and Hg 4f level (b) of CdS/HgS/CdS quantum dot quantum well nanocrystals as a function of kinetic energy. Experimental intensities are plotted together with simulated curves where the solid lines correspond to the best fit and the dashed lines serve for error estimation. The ratio of Hg to Cd is plotted in (c). The HgS well becomes more and more visible when the sampling depth is increased.

with the aim to determine the thickness of the different shells in the onion like nanocrystals.

A note is necessary here on the morphology of the samples. High resolution TEM measurements have shown that the CdS core particles may possess an approximately tetrahedral geometry which is partly maintained in the CdS/HgS/CdS quantum dot quantum well nanocrystals.[11] However, there are various defects such as truncated corners, twin grain boundaries, and edge dislocations which lead to numerous deviations from a regular tetrahedral shape.[11,27] Furthermore, because there are substantial deviations from a regular tetrahedral morphology anyway, we use a spherical model as simple approximation for the calculations.

Peak intensities of the Cd $3d_{5/2}$ and Hg 4f level have been measured at a series of energies and normalized as described above. In the case of the Hg 4f level, only the contribution of the component "V" associated with the quantum dot quantum well particles has been taken into account. Normalized experimental intensities are plotted as a function of the photoelectron kinetic energy in Figure 10, parts a and b.

For the simulation, the integral (1) is evaluated next. A spherical geometry is assumed and the diameter of the CdS core is fixed to 4.72 nm, because the initial CdS particles had a diameter of 5.3 nm according to the TEM images before the outermost layer of CdS was replaced by HgS. The thickness of the HgS shell and the outer CdS shell are a priori the variables in the simulation.

To perform numerical calculations the mean free path length has to be known. Tanuma, Powell, and Penn have developed a formula which takes into account several material parameters, namely, the density, the molecular weight, and total number of valence electrons per formula unit and the energy gap.[28] This formula allows calculation of the inelastic mean free path length as a function of energy in the different shells of the composite nanocrystals.

The outer layer of the stabilizing polyphosphates has also to be taken into account. Parameters used for calculations of the mean free path length in the stabilizer shell were 1.2 g/cm^3 for the density, 600 g/mol for the molecular weight, 180 valence electrons per formula unit, and 5 eV for the HOMO−LUMO gap. The calculation of the mean free path length cannot be considered as very accurate for the stabilizer shell, but it is the best possible attempt and should at least give the correct order of magnitude. Note also, that the results obtained for the thickness of the HgS and outer CdS shell were only very slightly dependent on reasonable variations of the parameters used for the stabilizer shell.

In a first attempt, we performed a layer thickness determination with the HgS and outer CdS shell thickness as independent variables. These calculations were however not conclusive. Good fits could be obtained over a wide range of values for the HgS shell thickness, because for each value we found a corresponding value for the outer CdS shell that more or less adjusted the simulated intensities. The method for shell thickness determination by photoelectron spectroscopy comes to its limits here.

However, it is still possible to perform reasonable calculations, if the total thickness of the HgS and outer CdS shell is fixed. According to the TEM images, both shells together have a thickness of 1.54 nm. The introduction of this constraint reduces the number of parameters in the simulation where now only the position of the border between the HgS and outer CdS shell is variable.

Under these conditions, the best fit is obtained with 0.60 nm for the HgS and 0.94 nm for the outer CdS shell thickness. The corresponding fitting curves are plotted as solid lines in Figure 10, parts a and b. The calculated ratio of the CdS shell thickness to the HgS shell thickness is 1.57 in good agreement with the expected value of 1.50 for 2 monolayers of HgS and 3 monolayers of CdS. A note may be necessary on the precision of the performed calculations. For computational reasons, all thickness parameters have been varied with a step size of 0.01 nm. Estimated errors for the results are larger however. The dashed lines in Figure 10, parts a and b, correspond to simulations with 0.55 and 0.65 nm for the HgS shell thickness and may be considered as error limits. A thickness ratio of 1.6 $\pm$ 0.2 for the two shells is the final result of the simulation method. For the stabilizer shell, the fitting procedure yields a thickness of 1.3 nm which seems also reasonable in its order of magnitude. Note again that these results correspond to a simple spherical structure model and can only be understood as average values.

3.6. Double Quantum Well Structure of CdS/HgS/CdS/HgS/CdS. The method for layer thickness determination turned out to be still applicable in the case of the quantum dot quantum well structure, if the constraint of fixing the combined thickness of the HgS and the outer CdS shell is introduced into the calculations. An extension of the method to the double quantum well structure seems unreasonable however. The only remaining possibility is here to simulate intensities for the ideal structure comprising of a CdS core and the 4 shells which are 2 monolayers of HgS, 3 monolayers of CdS, 2 monolayers of HgS, and finally 3 monolayers of CdS, respectively. The simulation of the ideal structure may then be compared to experimental intensities in order to test, if the experimental data is in accordance with the ideal structure.

Figure 11 shows normalized experimental intensities of the Cd $3d_{5/2}$ and Hg 4f level recorded from the double quantum well nanocrystals. Assuming identical parameters for the ligand shell as in the case of the quantum dot quantum well nanoparticles, theoretical intensities can easily be calculated. The only remaining free parameter in the calculations is a global constant

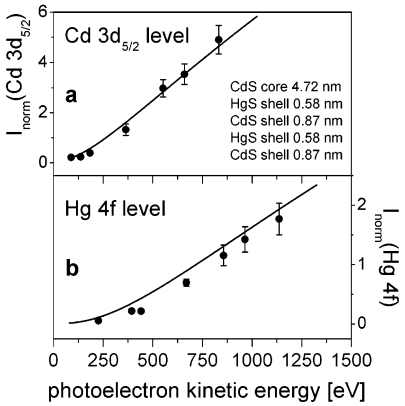

Figure 11. Normalized intensities of the Cd $3d_{5/2}$ (a) and Hg 4f level (b) of CdS/HgS/CdS/HgS/CdS nanocrystals as a function of kinetic energy. Experimental intensities are plotted together with a simulation of the ideal double quantum well structure.

of proportionality which has to be adjusted in order to take care of the actual concentration of nanocrystals on the substrate. The simulated curves are also plotted in Figure 11 and are roughly in agreement with the experimental data. Thus, the experimental intensities basically conform with the expectation for the ideal double quantum well structure. Any further layer thickness analysis does not seem possible here.

4. Summary and Conclusion

Quantum dot quantum well and double quantum well nanocrystals of CdS and HgS have been investigated by photoelectron spectroscopy with tuneable synchrotron radiation. As should be expected, high-resolution spectra are very similar for both structures. Spectra of the Cd $3d_{5/2}$ level show a second component shifted by about 0.4 eV to higher binding energy which can be assigned to the nanoparticle surface. Different sulfur species have not been resolved. In the case of mercury core level spectra, although not expected for the ideal structure model, there are two different species observed. About 10% of the total amount of Hg give evidence for sample inhomogeneities.

Furthermore, it has been shown that synchrotron XPS allows layer thickness analysis of the composite nanocrystals within certain limits. The method can be extended from core−shell nanocrystals to the CdS/HgS/CdS quantum dot quantum well structure, if the core diameter and the final particle size are fixed in the simulation. The calculations then confirm quite well the presence of 2 monolayers of HgS and 3 monolayers of again CdS grown on the CdS core particles.

Further extension of the method of layer thickness determination to the more complex case of the double quantum well nanocrystals does not appear to be possible. Nevertheless, we could successfully verify that the experimental photoemission intensities roughly conform with the ideal structure model of 2 monolayers of HgS, 3 monolayers of CdS, 2 monolayers of HgS, and finally 3 monolayers of CdS on the CdS core nanocrystals. Although a real layer thickness determination is not possible here anymore, the photoemission study at least supports the model of the double quantum well structure.

Acknowledgment. We thank A. Kornowski and S. Bartholdi-Nawrath for acquiring transmission electron micrographs. This work was supported by the German Science Foundation (DFG) within the framework of the SFB 508 and the DIP-D3.1.

References and Notes

(1) Weller, H. *Angew. Chem., Int. Ed*. **1993**, *32*, 41.
(2) Henglein, A. *Ber. Bunsen-Ges. Phys. Chem*. **1995**, *99*, 903.
(3) Eychmüller, A. *J. Phys. Chem. B* **2000**, *104*, 6514.
(4) Spanhel, L.; Haase, M.; Weller, H.; Henglein, A. *J. Am. Chem. Soc*. **1987**, *109*, 5649.
(5) Peng, X.; Schlamp, M. C.; Kadavanich, A. V.; Alivisatos, A. P. *J. Am. Chem. Soc*. **1997**, *119*, 7019.
(6) Hines, M. A.; Guyot-Sionnest, P. *J. Phys. Chem*. **1996**, *100*, 468.
(7) Talapin, D. V.; Rogach, A. L.; Kornowski, A.; Haase, M.; Weller, H. *Nano Lett*. **2001**, *1*, 207.
(8) Cao, Y. W.; Banin, U. *J. Am. Chem. Soc*. **2000**, *122*, 9692.
(9) Mews, A.; Eychmüller, A. *Ber. Bunsen-Ges. Phys. Chem*. **1998**, *102*, 1343.
(10) Eychmüller, A.; Mews, A.; Weller, H. *Chem. Phys. Lett*. **1993**, *208*, 59.
(11) Mews, A.; Kadavanich, A. V.; Banin, U.; Alivisatos, A. P. *Phys. Rev. B* **1996**, *53*, 13242.
(12) Braun, M.; Burda, C.; El-Sayed, M. A. *J. Phys. Chem. A* **2001**, *105*, 5548.
(13) Dorfs, D.; Eychmüller, A. *Nano Lett*. **2001**, *1*, 663.
(14) Winkler, U.; Eich, D.; Chen, Z. H.; Fink, R.; Kulkarni, S. K.; Umbach, E. *Phys. Stat. Sol. (A)* **1999**, *173*, 253.
(15) Winkler, U.; Eich, D.; Chen, Z. H.; Fink, R.; Kulkarni, S. K.; Umbach, E. *Chem. Phys. Lett*. **1999**, *306*, 95.
(16) Nanda, J.; Kuruvilla, B. A.; Sarma, D. D. *Phys. Rev. B* **1999**, *59*, 7473.
(17) Döllefeld, H.; McGinley, C.; Almousalami, S.; Möller, T.; Weller, H.; Eychmüller, A. *J. Chem. Phys*. **2002**, *117*, 8953.
(18) McGinley, C.; Riedler, M.; Möller, T.; Borchert, H.; Haubold, S.; Haase, M.; Weller, H. *Phys. Rev. B* **2002**, *65*, 245308.
(19) Borchert, H.; Haubold, S.; Haase, M.; Weller, H.; McGinley, C.; Riedler, M.; Möller, T. *Nano Lett.* **2002**, *2*, 151.
(20) McGinley, C.; Adam, S.; Möller, T.; Borchert, H.; Talapin, D. V.; Haase, M.; Weller, H.; de Castro, A. R. B. *Phys. Rev. B* submitted
(21) Borchert, H.; Talapin, D. V.; McGinley, C.; Adam, S.; de Castro, A. R. B.; Möller, T.; Weller, H. *J. Chem. Phys*. submitted
(22) Mews, A.; Eychmüller, A.; Giersig, M.; Schooss, D.; Weller, H. *J. Phys. Chem*. **1994**, *98*, 934.
(23) Seah, M. P.; Dench, W. A. *Surf. Interface Anal*. **1979**, *1*, 2.
(24) Heske, C.; Winkler, U.; Held, G.; Fink, R.; Umbach, E.; Jung, Ch.; Bressler, P. R.; Hellwig, Ch. *Phys. Rev. B* **1997**, *56*, 2070.
(25) Moretti, G.; Anichini, A.; Fierro, G.; LoJacono, M.; Porta, P. *Surf. Interface Anal*. **1990**, *16*, 352.
(26) Marychurch, M.; Morris, G. C. *Surf. Sci*. **1985**, *154*, L251.
(27) Lifshitz, E.; Porteanu, H.; Glozman, A.; Weller, H.; Pflughoefft, M.; Eychmüller, A. *J. Phys. Chem. B* **1999**, *103*, 6870.
(28) Tanuma, S.; Powell, C. J.; Penn, D. R. *Surf. Interface Anal*. **1993**, *21*, 165.